Sarah Mignot, Paolo Pellizzari and Frank Westerhoff*

Fake News and Asset Price Dynamics

https://doi.org/10.1515/jbnst-2024-0019
Received January 25, 2024; accepted June 24, 2024

Abstract: We explore the impact of fake news on asset price dynamics within the asset-pricing model of Brock and Hommes (Brock, W. A., and C. H. Hommes. 1998. "Heterogeneous Beliefs and Routes to Chaos in a Simple Asset Pricing Model." *Journal of Economic Dynamics and Control* 22 (8): 1235–74). By polluting the information landscape, fake news interferes with agents' perception of the dividend process of the risky asset. Our analysis reveals that fake news decreases the steady-state price of the risky asset by making it even more risky. Moreover, fake news increases the market share of agents who use the destabilizing technical trading rule by rendering fundamental trading more difficult and costly. Instead of converging toward its steady state, the risky asset's price may thus be subject to wild fluctuations. As it turns out, these fluctuations are concentrated below the risky asset's steady-state price. We also show that fake news campaigns may allow certain agents to realize fraudulent profits.

Keywords: asset price dynamics; fake news; chartists and fundamentalists; bounded rationality and learning; stability and bifurcation analysis

JEL Classification: G12; G14; G41

1 Introduction

We investigate the potential impact of the growing diffusion of fake news on the dynamics of financial markets, employing the influential asset-pricing model introduced by Brock and Hommes (1998) as our analytical framework. Fake news,

Article Note: This article is part of the special issue "Advancing Agent-based Economics" published in the Journal of Economics and Statistics. Access to further articles of this special issue can be obtained at www.degruyter.com/jbnst.

***Corresponding author: Frank Westerhoff**, Department of Economics, University of Bamberg, Feldkirchenstraße 21, 96045 Bamberg, Germany, E-mail: frank.westerhoff@uni-bamberg.de
Sarah Mignot, Department of Economics, University of Bamberg, Feldkirchenstraße 21, 96045 Bamberg, Germany
Paolo Pellizzari, Department of Economics, Ca' Foscari University of Venice, Venezia, Italy

broadly defined as false or misleading information presented as genuine, encompasses fabricated stories, distorted facts, and exaggerated claims. This deceptive content proliferates through various channels, including social media, websites, and traditional news outlets, with the overarching goal of manipulating public opinion. See Allcott and Gentzkow (2017), Lazer et al. (2018), Vosoughi, Roy, and Aral (2018), and Scheufele and Krause (2019) for comprehensive surveys on the subject of fake news. While Fama (1970) contends that asset prices reflect their underlying fundamentals, Black (1986) posits that certain speculators engage in trading based on noise, treating it as if it were information. This approach creates a disconnect between asset prices and their fundamental values. Shiller (2017) emphasizes the power of narratives, specifically popular stories, to go viral and spread globally, exerting a substantial influence on the economy. According to Shiller (2017), significant historical events such as the Great Depression, the Dotcom Bubble, and the Great Recession can be attributed to the prevailing narratives of their respective eras. The observations made by Kogan, Moskowitz, and Niessner (2023), who studied an undercover Securities and Exchange Commission (SEC) investigation into the manipulation of financial news on social media, are also noteworthy. They found that fake news has an impact on asset markets, driving prices, volatility, and trading volume.

Within the asset-pricing model by Brock and Hommes (1998), agents can invest in a safe asset and a risky asset. Although agents follow technical and fundamental expectation rules to predict the future price of the risky asset, their trading behavior ensures that the steady-state price of the risky asset is given by the discounted value of its future risk-adjusted dividend payments. Moreover, the price of the risky asset approaches its fundamental value, as long as the market share of agents who use the fundamental expectation rule is sufficiently large. However, agents' choice of expectation rules depends on the rules' past profitability. In addition, the fundamental expectation rule is more costly than the technical expectation rule, due to the need to analyze and process the fundamentals. As a result, the risky asset market may become unstable and display complex endogenous price fluctuations when the costs of using the fundamental expectation rule become too high. The asset-pricing model by Brock and Hommes (1998) has been extended in several directions. See Anufriev and Hommes 2012; Anufriev and Tuinstra 2013; Boswijk, Hommes, and Manzan 2007; Brock, Hommes, and Wagener 2009; Gaunersdorfer 2000; Gaunersdorfer and Hommes 2007; Gaunersdorfer, Hommes, and Wagener 2008; Hennequin and Hommes 2024; Hommes and in 't Veld 2017 for examples and Hommes (2006), Hommes and Wagener (2009), Hommes (2013), and Bao, Hommes, and Pei (2021) for reviews. To the best of our knowledge, however, no attempt has been made to adapt the framework to the presence of fake news.

In this paper, we explore how fake news may impact the dynamics of risky asset markets. We assume that fake news interferes with agents' perception of the risky asset's dividend process. In particular, fake news abnormally widens the perceived distribution of the dividend payments of the risky asset and, hence, increases its risk. Moreover, fake news also increases the costs associated with the fundamental expectation rule, as fundamentals themselves are blurred and more obscure in the presence of alternative news. Observe that this holds even if the fake news is unbiased and does not systematically distort prices in one direction. Using a mix of analytical and numerical tools, we establish the following results. First, fake news may depress the steady-state price of the risky asset. For agents to hold a constant supply of the risky asset in an environment in which fake news increases the uncertainty surrounding the risky asset, its steady-state price has to decrease. Second, fake news may inflate the steady-state market share of agents who rely on the technical expectation rule. Clearly, fake news makes fundamental trading more costly, which is why more agents may opt for technical trading. Third, an increase in the steady-state market share of the technical expectation rule may compromise the stability of the risky asset market. Once this happens, endogenous asset price dynamics set in.[1] Fourth, the transition between stable and unstable dynamics may be sharp, i.e. a small change in a model parameter may cause wild fluctuations of the risky asset's price. Due to the coexistence of calm and turbulent attractors, wild fluctuations may also be triggered by small exogenous shocks. Fifth, the price of the risky asset tends to fluctuate below the risky asset's steady-state price. This is caused by the risky asset's endogenous price dynamics, which amplifies the asset's riskiness. Recall that the steady-state price of the risky asset is already lower than the price in the absence of fake news. Hence the actual price of the risky asset truly suffers. Finally, fake news campaigns may allow certain agents to realize fraudulent profits, an aspect that policymakers should rigorously try to prevent.

Our paper is organised as follows. In Section 2, we develop our model setup, followed by a presentation of our analytical results in Section 3. After discussing our numerical results in Section 4, we conclude our paper in Section 5. Appendix A contains our main proofs. Some robustness checks are conducted in Appendix B.

2 Model Setup

In this section, we present our model setup, where we incorporate fake news in the seminal asset-pricing framework of Brock and Hommes (1998). In Sections 2.1–2.4, we

1 As we still see, endogenous asset price dynamics may include periodic, quasi-periodic, and chaotic price patterns.

discuss agents' trading environment, their variance and price beliefs, and their learning behavior.

2.1 Trading Environment and Asset Prices

Each agent i can either invest in a safe asset, paying a risk-free interest rate r, or in a risky asset, generating an uncertain dividend D_t as a payoff. The true dividend process of the risky asset is given by

$$D_t = \overline{D} + d_t, \tag{1}$$

where $\overline{D} > 0$ is a constant dividend component, and $d_t \sim \mathcal{N}(0, \sigma_d^2)$ are random dividend shocks. In this paper, we assume that the way in which agents perceive the dividend process is additively distorted by a fake news process F_t, i.e.

$$\widehat{D}_t = D_t + F_t, \tag{2}$$

where the fake news process follows

$$F_t = \overline{F} + f_t. \tag{3}$$

Parameter $\overline{F} \lesseqgtr 0$ denotes a (potentially) systematic misperception of dividend payments, while $f_t \sim \mathcal{N}\left(0, \sigma_f^2\right)$ reflects a random misperception of the dividend process. Assuming that D_t and F_t are independent, we are particularly interested in how parameters $\overline{F}$ and σ_f^2 of the fake news process influence the price dynamics of the risky asset.

Let us derive agents' demand for the risky asset. The end-of-period wealth of agent i, W_{t+1}^i, can be expressed as

$$W_{t+1}^i = \underbrace{(1+r)W_t^i}_{\text{safe asset}} + \underbrace{Z_t^i(P_{t+1} + D_{t+1} - (1+r)P_t)}_{\text{risky asset}}, \tag{4}$$

where Z_t^i denotes agent i's demand for the risky asset and P_t is the (ex-dividend) price of the risky asset. Agents are myopic mean-variance optimizers. Thus, agent i's demand for the risky asset solves the maximization problem

$$\max_{Z_t^i} E_t^i\left[W_{t+1}^i\right] - \frac{\lambda}{2} V_t^i\left[W_{t+1}^i\right], \tag{5}$$

where $\lambda > 0$ is a risk aversion parameter, assumed to be indentical for all agents.[2] From the first-order condition

2 As pointed out by an anonymous referee, it might be interesting to explore different trading behaviors in the future. For instance, the work by Epstein and Schneider (2008) suggests that when

$$E_t^i[P_{t+1}] + E_t^i[\widehat{D}_{t+1}] - (1+r)P_t - \lambda\Big(V_t^i[P_{t+1}] + V_t^i[\widehat{D}_{t+1}]\Big)Z_t^i = 0, \tag{6}$$

we obtain agent i's optimal demand for the risky asset

$$Z_t^i = \frac{E_t^i[P_{t+1}] + E_t^i[\widehat{D}_{t+1}] - (1+r)P_t}{\lambda\Big(V_t^i[P_{t+1}] + V_t^i[\widehat{D}_{t+1}]\Big).} \tag{7}$$

In total, there are N agents. Agents' expectations with respect to the risky asset's dividend payments are homogeneous and given by $E_t^i[\widehat{D}_{t+1}] = \overline{D} + \overline{F}$. Moreover, we assume that agents have identical variance beliefs, captured by $V_t^i[P_{t+1}] = \sigma_{P,t}^2$ and $V_t^i[\widehat{D}_{t+1}] = \sigma_d^2 + \sigma_f^2$. For ease of exposition, let the variance in the denominator of Z_t^i be

$$\sigma_t^2 = \sigma_{P,t}^2 + \sigma_d^2 + \sigma_f^2. \tag{8}$$

By denoting agents' average price expectation by $\frac{1}{N}\sum_{i=1}^{N} E_t^i[P_{t+1}] = E_t[P_{t+1}]$, we can express their aggregate demand for the risky asset as

$$Z_t = \sum_{i=1}^{N} Z_t^i = N\frac{E_t[P_{t+1}] + \overline{D} + \overline{F} - (1+r)P_t}{\lambda\sigma_t^2}. \tag{9}$$

Note that agents' aggregate demand for the risky asset increases in line with their price and dividend expectations, and decreases in line with the risk-free interest rate, the current price, risk aversion, and the perceived risk. While agents' aggregate demand increases (decreases) if parameter $\overline{F}$ increases (decreases), an increase in parameter σ_f^2 always decreases their desire to hold the risky asset.

Market clearing requires that demand and supply for the risky asset are equal, i.e.

$$Z_t = S_t. \tag{10}$$

The number of (outside) shares of the risky asset is constant and given by

$$S_t = \widehat{S} = N\overline{S}, \tag{11}$$

where $\overline{S}$ is the average number of available (outside) shares of the risky asset per agent.[3]

Combining (9), (10) and (11) reveals that the price of the risky asset is

ambiguity-averse agents process news of uncertain quality, they act as if they are taking a worst-case assessment of the quality. In such a setting, agents react more strongly to bad news than to good news and dislike assets for which information quality is poor, causing ambiguity premia and excess volatility. See also Bao, Duffy, and Zhu (2020) and Liang (2022).

3 Brock and Hommes (1998) assume a zero supply of (outside) shares of the risky asset. See Hommes, Huang, and Wang (2005), Anufriev and Tuinstra (2013), and Mignot, Tramontana, and Westerhoff (2021) for papers that also assume a positive supply of (outside) shares of the risky asset.

$$P_t = \frac{E_t[P_{t+1}] + \overline{D} + \overline{F} - \lambda\sigma_t^2\overline{S}}{1+r}. \tag{12}$$

This price, quite reasonably, increases in line with agents' price and dividend expectations, and decreases in line with the risk-free interest rate and the risk premium $\lambda\sigma_t^2\overline{S}$. Note that fake news influences the price of the risky asset via parameters $\overline{F}$ and σ_f^2. In particular, an increase in σ_f^2 depresses the price of the risky asset. The rationale behind this line of thought is that an increase in parameter σ_f^2 reduces agents' aggregate demand for the risky asset. In order for agents to hold the constant number of (outside) shares of the risky asset, its price has to decrease.

2.2 Homogeneous Variance Beliefs

As reported in (8), agents' variance beliefs comprise three components: a dividend component, a fake news component, and a price component. We follow Gaunersdorfer (2000) and model agents' beliefs about the variance of the risky asset's price as an exponential moving average. Agents update their perception of the price variance of the risky asset using a weighted average of past price variance perceptions and current squared deviations between the observed price of the risky asset and its average price U_t. Hence,

$$\sigma_{P,t}^2 = \upsilon\sigma_{P,t-1}^2 + (1-\upsilon)(P_{t-1} - U_{t-1})^2, \tag{13}$$

with $0 < \upsilon < 1$ as a memory parameter. The average price of the risky asset is also modeled as an exponential moving average and, similarly

$$U_t = \mu U_{t-1} + (1-\mu)P_{t-1} \tag{14}$$

is a weighted average of the past average price of the risky asset and the current observed price of the risky asset, where $0 < \mu < 1$ is a memory parameter.

2.3 Heterogeneous Price Beliefs

Agents use simple forecasting rules to predict the price of the risky asset. To keep the model analytically tractable, following Brock and Hommes (1998) we assume that agents switch between a fundamental expectation rule, denoted by $E_t^F[P_{t+1}]$, and a technical expectation rule, denoted by $E_t^C[P_{t+1}]$. Both expectation rules predict the price of the risky asset for period $t+1$ at the beginning of period t, relying on all the available information in period $t-1$. Agents' average expectation about the risky asset's price is defined as

$$E_t[P_{t+1}] = N_t^C E_t^C[P_{t+1}] + N_t^F E_t^F[P_{t+1}], \tag{15}$$

where N_t^C and N_t^F are the market shares of agents who follow the technical and the fundamental expectation rule, respectively. Note that (15) implies that the number of agents is large (technically speaking, there is a continuum of agents).

Agents who opt for the technical expectation rule, called chartists, predict that the risky asset's current price trend will continue. Their expectation rule is formalized by

$$E_t^C[P_{t+1}] = P_{t-1} + \chi(P_{t-1} - P_{t-2}), \tag{16}$$

where $\chi > 0$ is the strength of extrapolative behavior.

Agents who use the fundamental expectation rule, called fundamentalists, believe that the price of the risky asset will revert to its fundamental value. Their expectation rule is formalized by

$$E_t^F[P_{t+1}] = P_{t-1} + \phi\left(P_{t-1}^\star - P_{t-1}\right), \tag{17}$$

where $0 < \phi < 1$ is the expected mean reversion speed.

Market participants estimate the fundamental value of the risky asset by discounting (perceived) risk-adjusted dividend payments

$$P_t^\star = \frac{\overline{D} + \overline{F} - \lambda\sigma_t^2\overline{S}}{r}. \tag{18}$$

Note that this solution follows from (12) by assuming that $P_t = E_t[P_{t+1}] = P_t^\star$. In the absence of endogenous price dynamics, agents' fundamental value perception of the risky asset is given by

$$P^\star = \frac{\overline{D} + \overline{F} - \lambda\left(\sigma_d^2 + \sigma_f^2\right)\overline{S}}{r}. \tag{19}$$

Finally, the true fundamental value of the risky asset equals

$$P^v = \frac{\overline{D} - \lambda\sigma_d^2\overline{S}}{r}. \tag{20}$$

In our setup, agents' steady-state perception of the fundamental value of the risky asset may obviously be biased due to parameters $\overline{F}$ and σ_f^2.

2.4 Market Shares and Learning Behavior

The market shares of chartists and fundamentalists depend on the difference in the expectation rule's fitness, denoted by A_t^C and A_t^F, respectively. The market share of chartists is defined as

$$N_t^C = \frac{\exp\left[\beta A_t^C\right]}{\exp\left[\beta A_t^C\right] + \exp\left[\beta A_t^F\right]} = \frac{1}{1 + \exp\left[\beta\left(A_t^F - A_t^C\right)\right]}, \tag{21}$$

while the market share of fundamentalists is defined as

$$N_t^F = 1 - N_t^C. \tag{22}$$

The intensity of choice parameter $\beta > 0$ indicates how quickly the mass of agents switches to the forecasting rule with the highest fitness. If $\beta = 0$, then agents do not consider any difference in the fitness of their expectation rules and, being $N_t^C = N_t^F = \frac{1}{2}$, agents are equally divided between extrapolative and fundamental behavior. Clearly, this corresponds to an extreme situation in which all agents randomly pick their expectation rule. As β tends to infinity, then any difference in the fitness of their expectation rules is taken into account, and all agents opt for the expectation rule with the highest fitness.

As proposed by Gaunersdorfer, Hommes, and Wagener (2008), we assume that fitness is measured by risk-adjusted profits. If net profits seem to be a first natural fitness candidate, using risk-adjusted profits is consistent with agents' mean-variance optimization behavior. Thus, the fitness of the technical expectation rule is equal to

$$A_t^C = \underbrace{(P_{t-1} + D_{t-1} - (1+r)P_{t-2})Z_{t-2}^C}_{\text{realized profit}} - \underbrace{\frac{\lambda}{2}\sigma_{t-2}^2\left(Z_{t-2}^C\right)^2}_{\text{risk adjustment}}. \tag{23}$$

For the fitness of the fundamental expectation rule, we naturally consider two additional components. First, we take into account an economic indicator, increasing the fitness if agents observe an increase in mispricing, which asserts that the fitness of the fundamental expectation rule increases in line with the mispricing of the risky asset. Clearly, agents believe more strongly in mean reversion when the price of the risky asset is at a distance from its fundamental value.[4] Second, we consider a time-varying cost term in order to capture the expenditures associated with fundamental trading, which, as just seen, is more sophisticated and demanding than the straightforward use of technical expectation rules. Together, this yields

$$A_t^F = \underbrace{(P_{t-1} + D_{t-1} - (1+r)P_{t-2})Z_{t-2}^F}_{\text{realized profit}} - \underbrace{\frac{\lambda}{2}\sigma_{t-2}^2\left(Z_{t-2}^F\right)^2}_{\text{risk adjustment}} + \underbrace{\alpha\left(P_{t-1} - P_{t-1}^*\right)^2}_{\text{mispricing}} - \underbrace{C_{t-1}}_{\text{costs}}, \tag{24}$$

4 See also Gaunersdorfer (2000), Gaunersdorfer and Hommes (2007), and Franke and Westerhoff (2012).

where parameter $\alpha > 0$ controls the strength of the mispricing effect. The demand of chartists and fundamentalists at time $t-2$ is given by

$$Z_{t-2}^{C} = \frac{E_{t-2}^{C}[P_{t-1}] + \overline{D} + \overline{F} - (1+r)P_{t-2}}{\lambda \sigma_{t-2}^{2}} \tag{25}$$

and

$$Z_{t-2}^{F} = \frac{E_{t-2}^{F}[P_{t-1}] + \overline{D} + \overline{F} - (1+r)P_{t-2}}{\lambda \sigma_{t-2}^{2}}, \tag{26}$$

respectively.

We assume that it becomes increasingly costly for agents to act as fundamentalists when the uncertainty surrounding the risky asset increases. Roughly speaking, these costs should be proportional to σ_t^2. However, to distinguish the effect of the model's different risk components on the dynamics of the risky asset's market, we prefer the following formalization

$$C_t = c_1 \sigma_d^2 + c_2 \sigma_f^2 + c_3 \sigma_{P,t}^2, \tag{27}$$

where c_1, c_2, and c_3 are positive parameters. The first term of (27) reflects costs that originate from the randomness of the true dividend process. Essentially, this type of costs is also reflected in the seminal asset-pricing model by Brock and Hommes (1998). The second term of (27) represents additional costs that arise from the risk associated with the fake news process. The higher the volatility of fake news, i.e. the higher parameter σ_f^2, the more costly it is to act as a fundamentalist. Note that while policymakers may attenuate these costs by reducing parameter c_2, for example, through a counter-information campaign, it is clearly difficult to act against a flow of inaccurate, sensationalist, and misleading information about the fair value and prospects of listed firms. For a good introduction and data, see EUvsDisinfo (2023). The third term of (27) reflects the costs associated with the endogenous behavior of the risky asset's price. The more volatile the price of the risky asset, the more difficult it is to follow the fundamental expectation rule.

3 Analytical Results

In this section, we discuss our analytical results. In particular, we are interested in how an increase in the intensity of fake news affects the steady-state price of the risky asset, agents' steady-state distribution across expectation rules, and the local stability of the risky asset market.

The following proposition, proven in Appendix A, summarizes our insights.

Proposition 1: *The deterministic skeleton of our model is driven by a 10-dimensional nonlinear map. This map possesses a unique steady state at which*

$$\overline{P} = P^* = \overline{U} = \frac{\overline{D} + \overline{F} - \lambda\left(\sigma_d^2 + \sigma_f^2\right)\overline{S}}{r}, \quad \overline{\sigma_P^2} = 0$$

and

$$\overline{N^C} = \frac{1}{1 + \exp\left[-\beta\left(c_1\sigma_d^2 + c_2\sigma_f^2\right)\right]}.$$

For $\chi < 1 + r$, the model's steady state is locally stable, while for $\chi > 2(1 + r)$, its steady state is unstable. For $1 + r < \chi < 2(1 + r)$, the model's steady state is locally stable if and only if $\beta\left(c_1\sigma_d^2 + c_2\sigma_f^2\right) < \log\left[\frac{1+r}{\chi-(1+r)}\right]$. A violation of this condition is associated with a Neimark-Sacker bifurcation.

Let us discuss the main economic implications of Proposition 1.

- **Steady state**: Fake news may affect the model's steady state as follows. An increase (decrease) in parameter $\overline{F}$ increases (decreases) the steady-state price of the risky asset. For instance, if agents overestimate the risky asset's dividend payments due to $\overline{F} > 0$, then the asset's steady-state is overvalued. Remarkably, however, even if fake news injects no systematic bias in the mean perception of the risky asset's dividend payments, i.e. $\overline{F} = 0$, an increase in parameter σ_f^2 inflates the risk premium of the risky asset and therefore decreases its steady-state price. Moreover, an increase in parameter σ_f^2 raises the costs of acting as a fundamentalist, and thus boosts the steady-state market share of chartists.
- **Local stability**: Fake news may destabilize the nature of the steady state of our model. As shown in Appendix A, the steady state's local stability condition requires that $\overline{N^C}\chi < 1 + r$ from which we can derive the following conclusions. For $\beta = 0$, we have $\overline{N^C} = \overline{N^F} = \frac{1}{2}$. Thus, if $\chi > 2(1 + r)$, then the steady state is unstable. For $\beta \to \infty$, we have $\overline{N^C} \to 1$ and $\overline{N^F} \to 0$. Thus, if $\chi < 1 + r$, then the steady state is locally stable. For $1 + r < \chi < 2(1 + r)$, we can deduce from Proposition 1 that an increase in $\beta\left(c_1\sigma_d^2 + c_2\sigma_f^2\right)$ might compromise the local stability of the steady state via a Neimark–Sacker bifurcation. In fact, an increase in $\beta\left(c_1\sigma_d^2 + c_2\sigma_f^2\right)$ causes an increase in $\overline{N^C}$, and thus chartists' destabilizing market impact becomes too strong. To be more precise, an increase in parameter β makes it more likely at the steady-state that agents will opt for the technical expectation rule, which has a higher fitness due to lower costs. Parameters σ_d^2 and σ_f^2 increase the risky asset's uncertainty and the costs related to the

fundamental rule. However, a decrease in parameter c_1 and/or c_2 might re-establish the steady state's local stability. Likewise, we can deduce from Proposition 1 that an increase in $\frac{1+r}{\chi-(1+r)}$ makes it more unlikely that the local stability of the steady state becomes compromised via a Neimark–Sacker bifurcation. While a higher extrapolation strength χ is harmful for the local stability of the steady state, a higher interest rate r is beneficial for the steady state's local stability.

As we will see in the next section, we may observe the emergence of endogenous asset price dynamics when the Neimark–Sacker bifurcation occurs. However, the Neimark–Sacker bifurcation may be supercritical or subcritical. In the former case, we will see that the risky asset market becomes unstable at the Neimark–Sacker bifurcation and that the amplitude of the risky asset's price dynamics gradually increases in line with parameter σ_f^2. In the latter case, it seems that the Neimark–Sacker bifurcation may be accompanied by a Chenciner bifurcation, i.e. our model may give rise to coexisting attractors before the Neimark–Sacker bifurcation occurs.[5] For initial values in the neighborhood of the steady state, we may observe stable asset price dynamics, whereas for initial conditions at a greater distance from the steady state, we may observe endogenous asset price fluctuations. Such cycles may emerge with a significant amplitude. All the previous analytical results support the economic intuition that fake news may not only depress the price of the risky asset, even if no systematic bias is added, through the additional risk perceived by mean-variance traders, but can also ignite episodes of wide endogenous fluctuations described by the bifurcations mentioned above.

4 Numerical Results

In this section, we numerically illustrate the model's analytical properties and study its out-of-equilibrium behavior. In Section 4.1, we introduce our base parameter setting. In Sections 4.2–4.5, we discuss different cases of fake news. Finally, we simulate the effects of a number of different fake news campaigns in Section 4.6.

4.1 Base Parameter Setting

Table 1 presents our base parameter settings. Some parameter values have been adopted from Brock and Hommes (1998), while others have been selected to best

5 The dimension of our model precludes an analytival treatment of the Chenciner bifurcation.

Table 1: Parameter setting.

Parameter	Economic meaning
$r = 0.1$	Interest rate
$\overline{D} = 10$	Mean dividend payment
$\overline{F} = 0$	Mean misperception
$\lambda = 0.1$	Risk aversion parameter
$\overline{S} = 1$	Average number of (outside) shares
$\sigma_d^2 = 2$	Variance of the dividend process
$\sigma_f^2 = 5$	Variance of the fake news process
$\upsilon = 0.9$	Memory parameter price volatility
$\mu = 0.9$	Memory parameter average price
$\chi = 1.2$	Strength of extrapolative behavior
$\phi = 0.8$	Expected mean reversion speed
$\beta = 1$	Intensity of choice parameter
$\alpha = 1$	Misalignment parameter
$c_1 = 0.5$	Costs parameter dividend process
$c_2 = 0.5$	Costs parameter fake news process
$c_3 = 0.5$	Costs parameter price volatility

visualize the effects of fake news. Accordingly, the steady-state price of the risky asset is equal to $\overline{P} = 93$. Since the market share of agents using the extrapolative expectation rule is given by $\overline{N^C} \approx 0.97$, it follows from Proposition 1 that the steady state of our model is unstable.[6]

To explain the functioning of our model, we consider four cases of fake news, summarized in Table 2. In Case I, we only restrict our attention on a single channel of propagation of fake news, namely the impact of parameter σ_f^2 on the risky asset's variance σ_t^2. To put it differently, Case I rests on the assumption that $c_2 = c_3 = \sigma_{P,t}^2 = 0$. In Case II, we additionally consider the parametrization where fake news increases the costs of being a fundamentalist. This effect could be controlled via parameter c_2. In Case III, we add to our analysis the parametrization where agents' update their variance beliefs via the price dynamics of the risky asset, permitting $\sigma_{P,t}^2$ to be positive. Case IV covers our entire model, i.e. we there also consider the parametrization where the costs of being a fundamentalist depend on the variance of the risky asset's price. This link is established via parameter c_3. Clearly, the parameters presented in Table 1 apply to Case IV. In Case

6 For $\sigma_f^2 = 0$, we have that $\overline{P} = 98$ and $\overline{N^C} \approx 0.73$. In the abscence of fake news, the steady state of our model is locally stable.

Table 2: Four cases of fake news.

Parameter	Case I	Case II	Case III	Case IV
σ_f^2	+	+	+	+
c_2	0	+	+	+
$\sigma_{P,t}^2$	0	0	+	+
c_3	0	0	0	+

I, II, and III, some of these parameters are set to zero, as previously discussed. See Appendix B for some additional simulations.

4.2 Case I

In Case I, we consider the parametrization where fake news only affects agents' variance beliefs via parameter σ_f^2, i.e. we set $c_2 = 0$, $c_3 = 0$, and $\sigma_{P,t}^2 = 0$. Figure 1 shows two bifurcation diagrams in which we depict the risky asset's price (left panel) and the market share of chartists (right panel) versus parameter σ_f^2. Since $c_2 = 0$, parameter σ_f^2 has no influence on the level of chartists' market share, which remains constant at $\overline{N^C} \approx 0.73$. As it is already clear from Proposition 1, parameter σ_f^2 does not

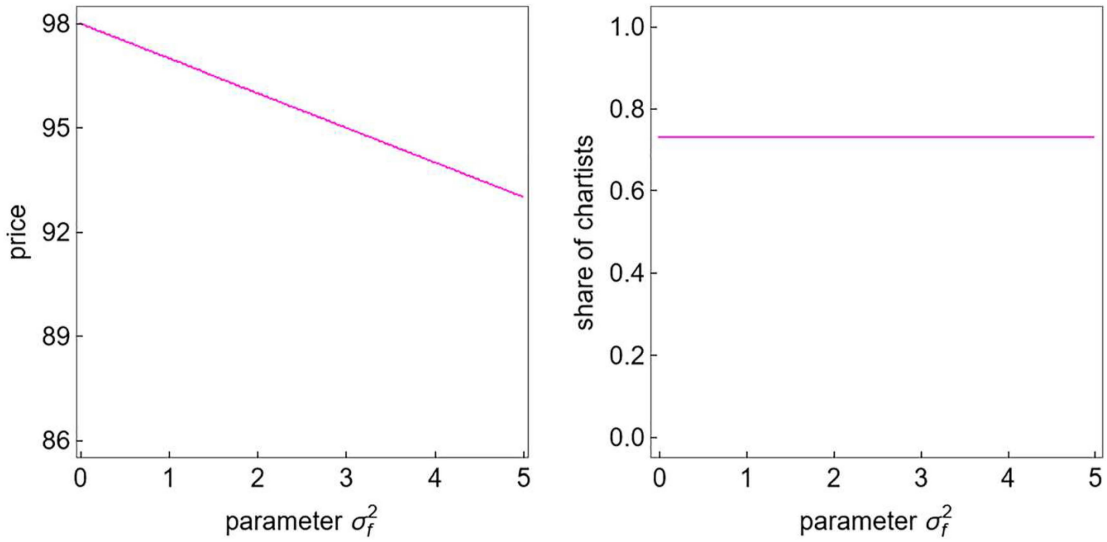

Figure 1: Case I. The left panel shows a bifurcation diagram in which the risky asset's price is depicted versus parameter σ_f^2. The right panel shows a bifurcation diagram in which the market share of chartists is depicted versus parameter σ_f^2.

constrain the local stability of the steady state. However, the price of the risky asset decreases in line with parameter σ_f^2, namely from 98 to 93. In fact, an increase in parameter σ_f^2 decreases agents' demand for the risky asset due to an increase in perceived risk. To then in return hold the constant number of (outside) shares of the risky asset, its price has to decrease.

4.3 Case II

In Case II, we assume that agents' variance beliefs and the costs of using the fundamental expectation rule are independent of the risky asset's price variance, i.e. we set $\sigma_{P,t}^2 = 0$ and $c_3 = 0$. Figure 2 presents our results.

As it can be seen from the bifurcation diagram in the bottom-left panel, the market share of chartists increases in line with parameter σ_f^2 and, consequently, constrains the local stability of the steady state. The steady state loses its local stability for $\sigma_f^2 \approx 2.796$, at which $\overline{N^C} \approx 0.917$. At this point, as it is visible from the bifurcation diagram depicted in the top-left panel, endogenous asset price dynamics set in. As is typical for a supercritical Neimark–Sacker bifurcation, the amplitude of the dynamics is initially small and then increases in line with the bifurcation parameter. In the top-right panel, we depict the evolution of the risky asset's price in the time domain. The price of the risky asset oscillates around its steady-state value $\overline{P} = 93$, represented by the dashed green line. The bottom-right panel presents the dynamics of our model in the (P_{t+1}, P_t) state space. The emergence of an invariant circle with periodic and quasiperiodic dynamics (purple ring) is typical for cyclical dynamics. The green dot marks the position of the risky asset's steady-state price.

4.4 Case III

In Case III, we assume that agents' perception of price variance has no impact on the costs of using the fundamental expectation rule, i.e. we set $c_3 = 0$. Figure 3 presents our results.

As it is clear from the bottom-left panel, the steady state loses its stability via a supercritical Neimark-Sacker bifurcation at the same value of parameter σ_f^2 as in Case II. Here, however, the risky asset's average price fluctuates ceteris paribus at a lower level (top-left panel). Note also that the market share of chartists definitely drops to lower levels in some cases (bottom-left panel). The top-right panel shows the

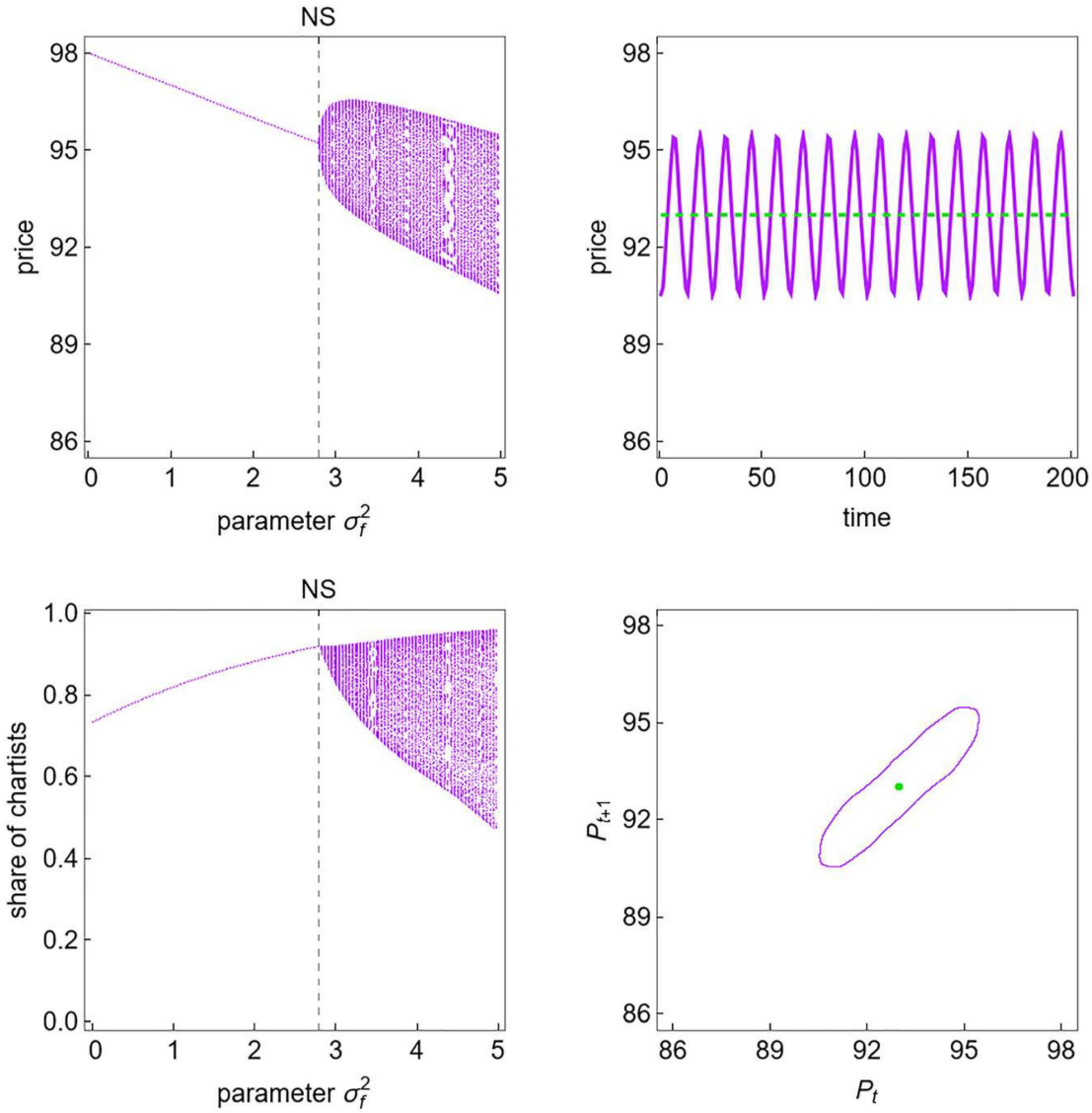

Figure 2: Case II. The top-left panel shows a bifurcation diagram in which the risky asset's price is depicted versus parameter σ_f^2. The bottom-left panel shows a bifurcation diagram in which the market share of chartists is depicted versus parameter σ_f^2. The top-right panel shows the evolution of the risky asset's price in the time domain. The bottom-right panel shows the risky asset's price in period t versus its price in period $t + 1$.

evolution of the price of the risky asset in the time domain, with the dashed green line representing the steady-state price, the orange dashed line indicating the average price, and the gray line depicting the perceived fundamental value. Unlike in Case II, the perceived fundamental value fluctuates around an average of 90.86, at a lower level than the steady-state price $\overline{P} = 93$, since agents' perception of price variance of the risky asset increases its risk premium.

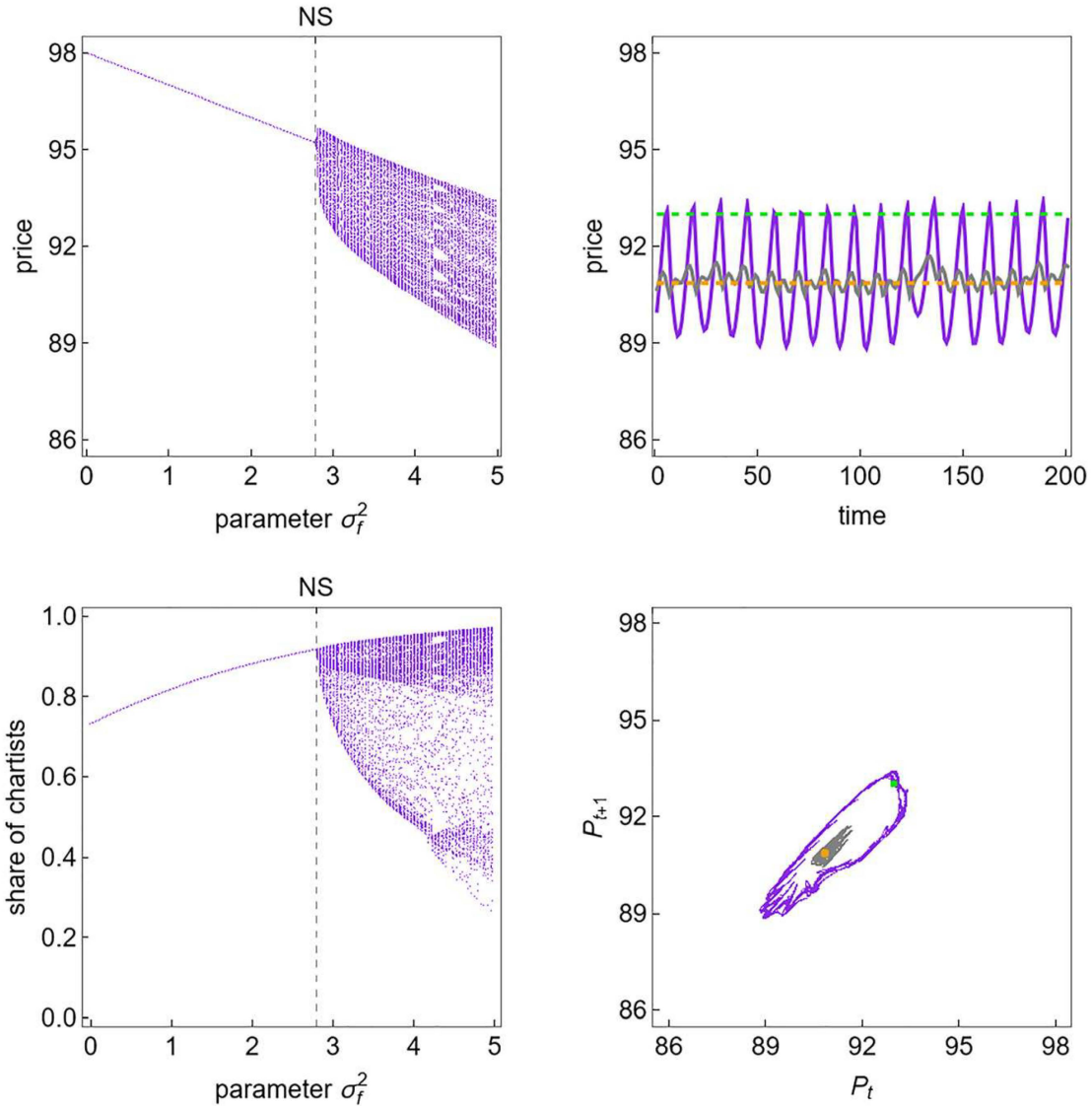

Figure 3: Case III. The top-left panel shows a bifurcation diagram in which the risky asset's price is depicted versus parameter σ_f^2. The bottom-left panel shows a bifurcation diagram in which the market share of chartists is depicted versus parameter σ_f^2. The top-right panel shows the evolution of the risky asset's price in the time domain. The bottom-right panel shows the risky asset's price in period t versus its price in period $t + 1$.

4.5 Case IV

Case IV, portrayed in Figure 4, reflects the dynamics of our full model.

Again, the steady state loses its local stability at the same value of parameter σ_f^2, as in Cases II and III. Differently from Case III, the transition between stable dynamics and endogenous fluctuations occurs abruptly (left panels) and the model's dynamics becomes more irregular (right panels). Obviously, a tiny change in one of

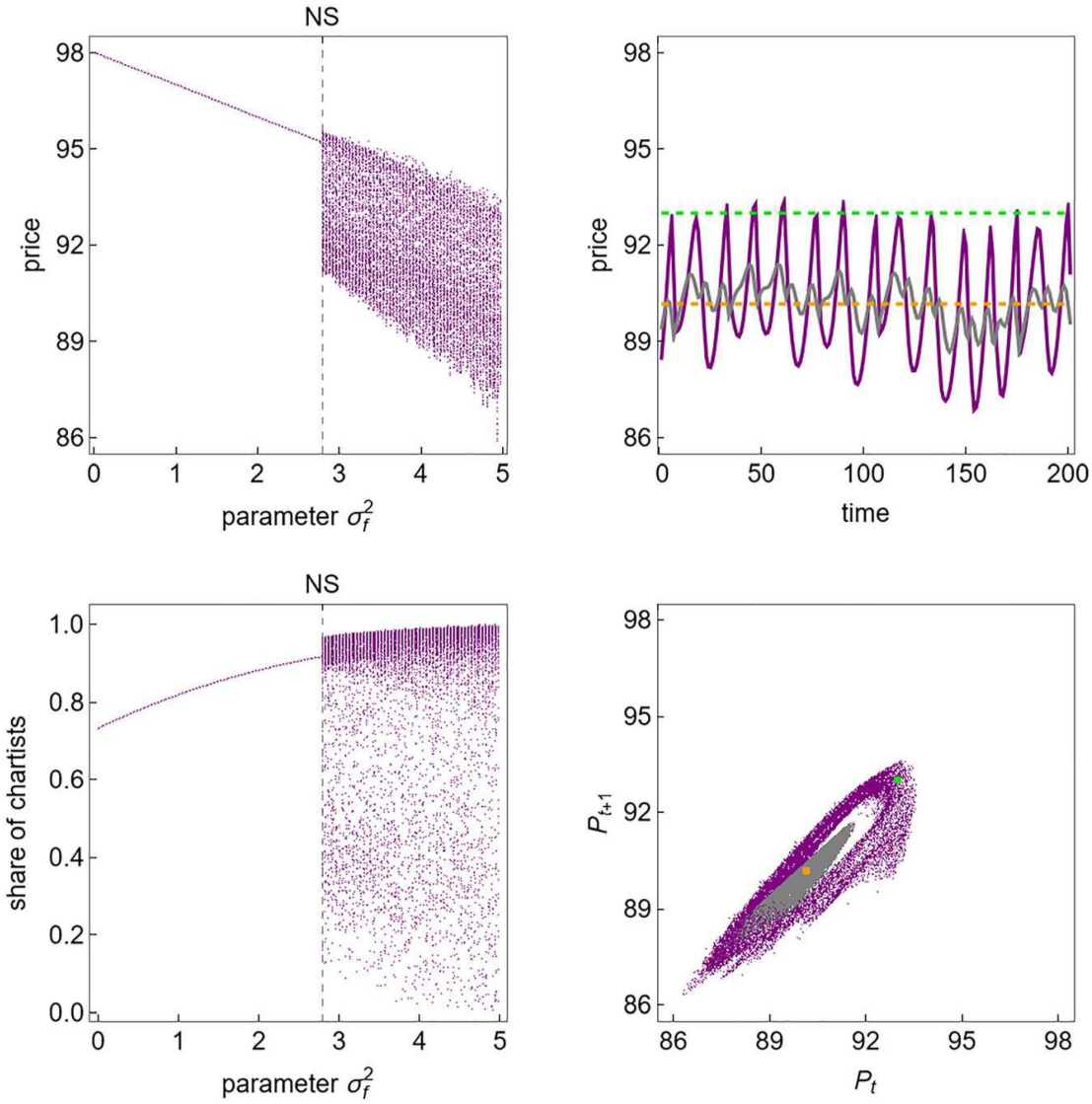

Figure 4: Case IV. The top-left panel shows a bifurcation diagram in which the risky asset's price is depicted versus parameter σ_f^2. The bottom-left panel shows a bifurcation diagram in which the market share of chartists is depicted versus parameter σ_f^2. The top-right panel shows the evolution of the risky asset's price in the time domain. The bottom-right panel shows the risky asset's price in period t versus its price in period $t + 1$.

the model's parameter may have a drastic effect on the behavior of the risky asset's market. Figure 4 suggests that we now observe a subcritical Neimark–Sacker bifurcation accompanied by a Chenciner bifurcation.[7]

Figures 5 and 6 explore this issue in more detail. Let us start with Figure 5. The left panel shows a bifurcation diagram in which the price of the risky asset is plotted

7 See also Agliari (2006), Gaunersdorfer, Hommes, and Wagener (2008), Neugart and Tuinstra (2003), and Lines and Westerhoff (2010, 2012).

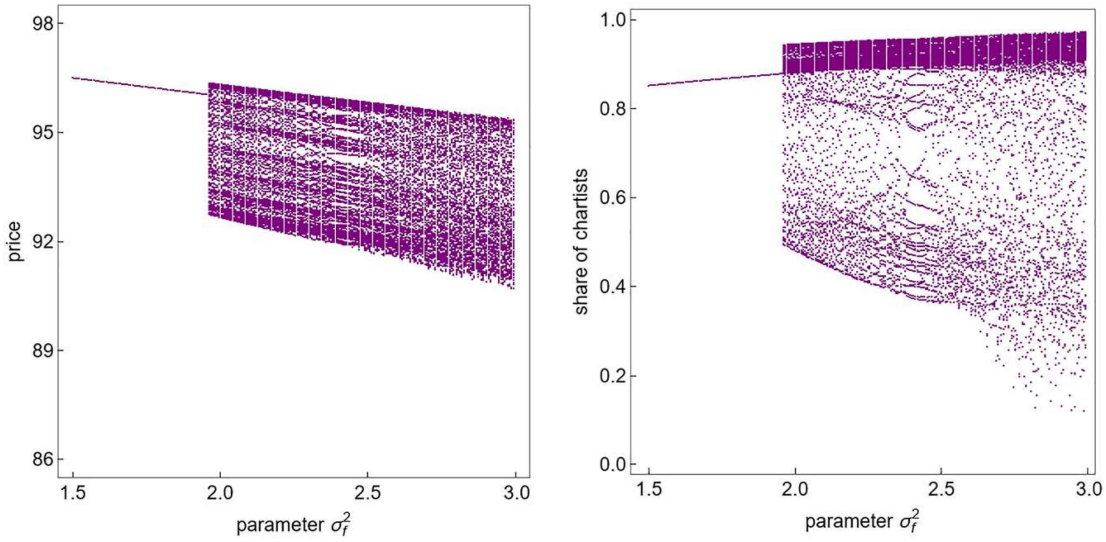

Figure 5: Bifurcation diagrams. The left (right) panel shows a bifurcation diagram in which the risky asset's price (the market share of chartists) is depicted versus parameter σ_f^2 for an initial value of $P_0 = \overline{P} + 2$. All other state variables correspond to their steady-state values.

against parameter σ_f^2, and the right panel shows a bifurcation diagram in which the market share of chartists is plotted against parameter σ_f^2. In contrast to the bifurcation diagrams reported in Figure 4, however, this time we have selected initial conditions that are at a greater distance from our model's steady state. As a result, endogenous fluctuations now set in at $\sigma_f^2 \approx 1.959$ instead of at $\sigma_f^2 \approx 2.796$.

Let us now turn to Figure 6. The top-left panel shows the evolution of the price of the risky asset in the time domain for $\sigma_f^2 = 2.75$. Clearly, the risky asset market may even display endogenous dynamics before the Neimark–Sacker bifurcation occurs. The top-right panel shows a basin of attraction plot for $\sigma_f^2 = 2.75$. Here we vary P_0 and X_0 as initial values on the axis.[8] All other state variables correspond to their steady-state values. The light purple area visualizes initial value combinations that converge toward the model's steady state. Note that there exists a "small" area around the steady state, yielding a convergence toward the model's steady state. However, there are also combinations that are more distant from the model's steady state, which produce stable dynamics. The cyan colored area visualizes initial value combinations that generate endogenous dynamics, as portrayed in the top-left panel. The pink colored area represents initial value combinations for which the model's dynamics is divergent.

Obviously, the coexistence of attractors allows intriguing attractor switching dynamics in the presence of (occasional) random disturbances. For instance, even a

8 Note that $P_t = X_{t-1}$.

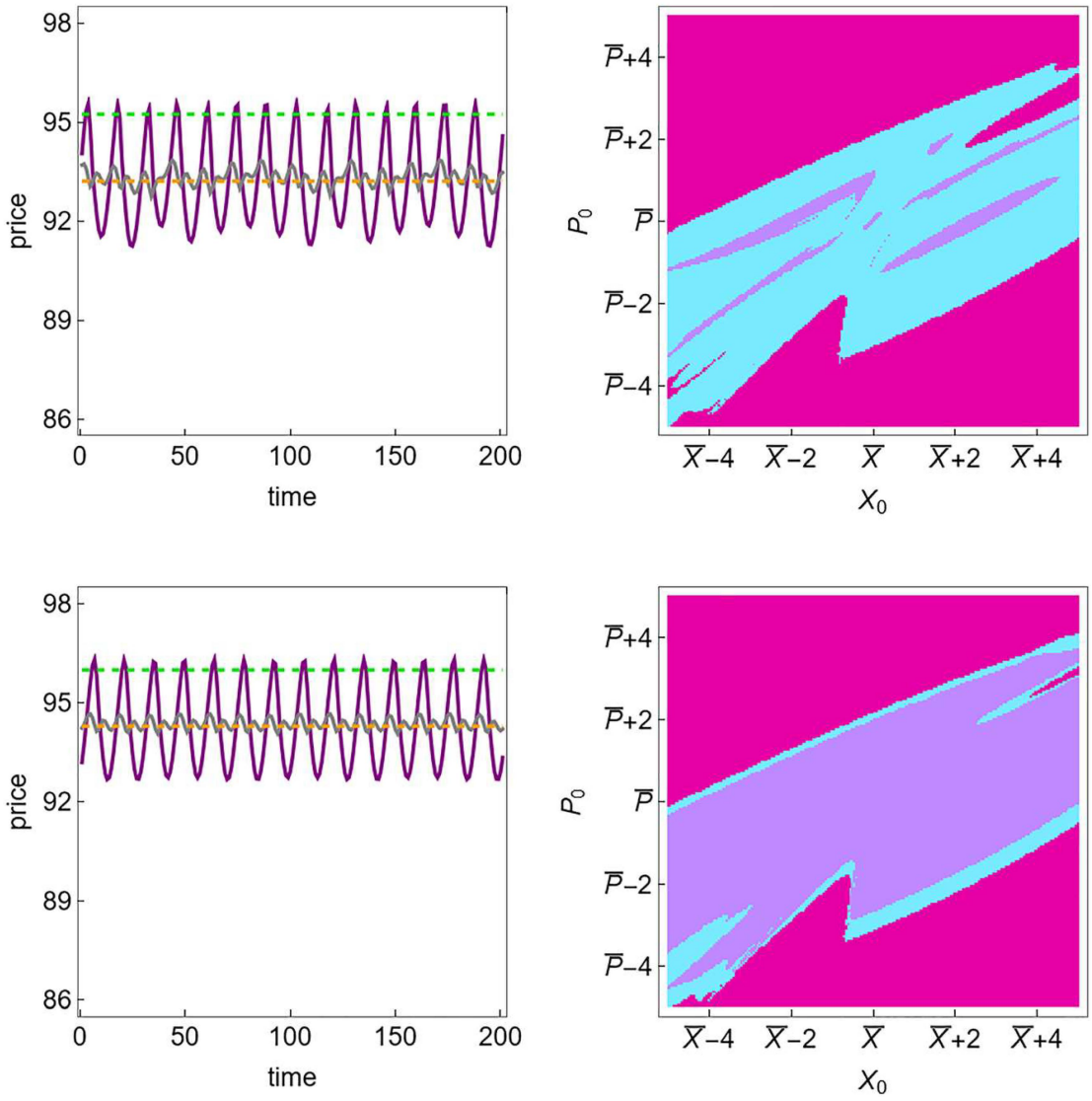

Figure 6: Basins of attraction. The top-left (bottom-left) panel shows the evolution of the risky asset's price in the time domain for an initial value of $P_0 = \overline{P} + 2$ and $\sigma_f^2 = 2.75$ $\left(\sigma_f^2 = 2.00\right)$. The top-right (bottom-right) panel shows the basin of attraction for $\sigma_f^2 = 2.75$ $\left(\sigma_f^2 = 2.00\right)$ for different combinations of initial value (X_0, P_0). All other state variables correspond to their steady-state values.

tiny exogenous shock may force the system out of the basin of attraction that yields stable dynamics, resulting in a volatility outburst. The bottom-left panel shows the evolution of the price of the risky asset in the time domain for $\sigma_f^2 = 2.00$. It becomes clear that endogenous dynamics might occur "well" before the Neimark–Sacker bifurcation. The bottom-right panel shows a basin of attraction plot for $\sigma_f^2 = 2.00$. Once more, the light purple area, the cyan area, and the pink area correspond to convergent, endogenous, and divergent dynamics, respectively. If the area of initial value combinations converging toward the model's steady state has increased

compared to $\sigma_f^2 = 2.75$, there are still initial value combinations that generate endogenous dynamics.[9]

4.6 Fake News Campaigns

In this section, we study the consequences of a number of different fake news campaigns, depicted in Figures 7 and 8. According to the empirical evidence provided by Arcuri, Gandolfi, and Russo (2023), Kogan, Moskowitz, and Niessner (2023), and Karppi and Crawford (2016), fake news campaigns may have an impact on risky asset markets, manipulating prices, volatility, and trading volume.

In the left panel of Figure 7, we assume that a fake news campaign initially manages to gradually increase parameter $\overline{F}$ from 0 to 0.5 between $t = 251$ and 500. Between $t = 501$ and 750, however, the fake news campaign ebbs away and parameter $\overline{F}$ gradually decreases from 0.5 to 0. Parameter σ_f^2 is equal to 3. Obviously, fake news campaigns may create bubbles. Provided that the costs of fake news campaigns are

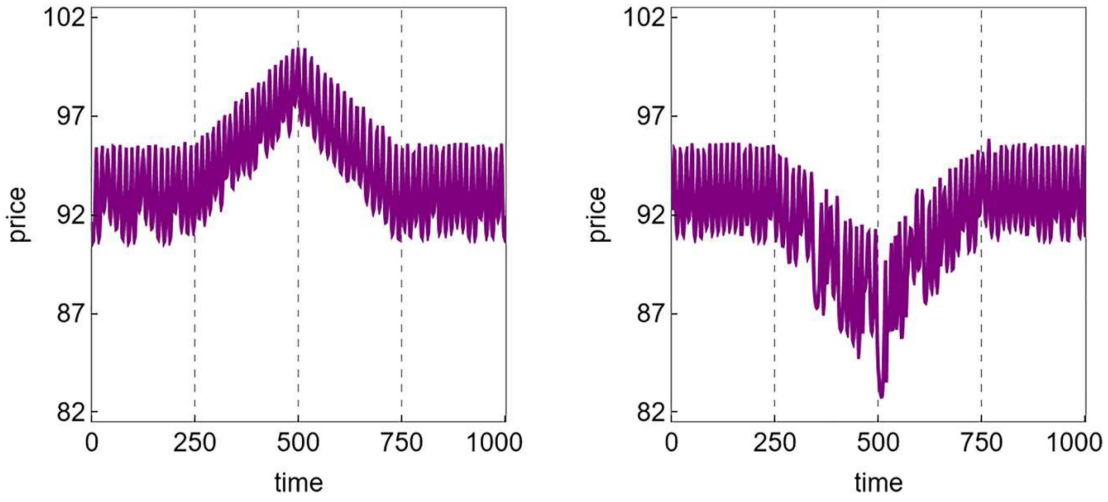

Figure 7: The impact of fake news campaigns. The panels show the evolution of the risky asset's price for different fake news campaigns in the time domain. Left panel: Between $t = 251$ and 500, parameter $\overline{F}$ gradually increases from 0 to 0.5. Between $t = 501$ and 750, parameter $\overline{F}$ gradually decreases from 0.5 to 0. Parameter σ_f^2 is equal to 3. Right panel: Between $t = 251$ and 500, parameter σ_f^2 gradually increases from 3 to 7. Between $t = 501$ and 750, parameter σ_f^2 gradually decreases from 7 to 3. Parameter $\overline{F}$ is equal to 0.

9 Once again: a word of caution is in order. The dynamics of our model is driven by the iteration of a 10-dimensional nonlinear map. The projection of the basins of attraction visible here only cover two dimensions.

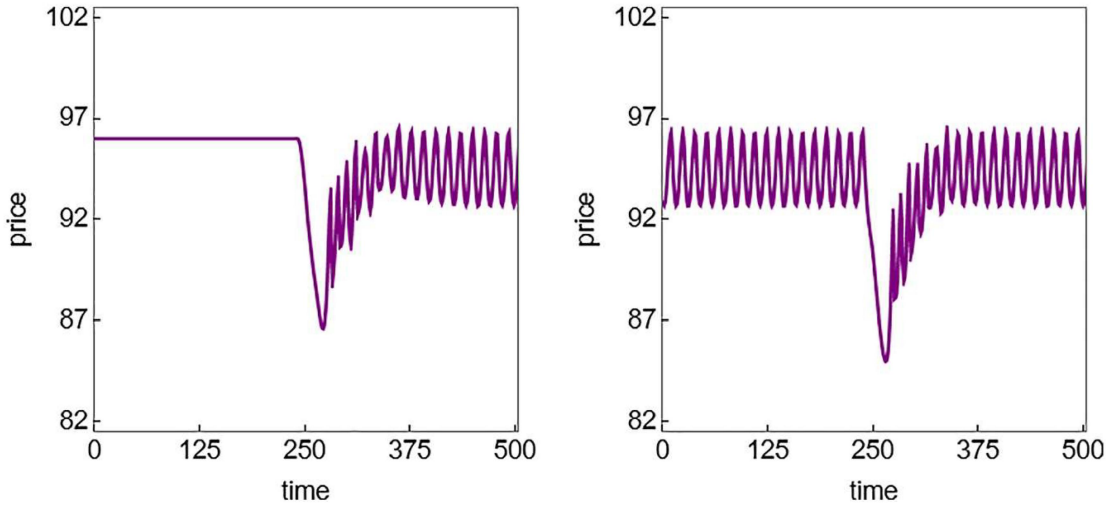

Figure 8: Abrupt (flash) crashes and fake news campaigns. The panels show the evolution of the risky asset's price for different fake news campaigns in the time domain, assuming that parameter σ_f^2 is equal to 2. Left panel: Between t = 241 and 250, parameter $\overline{F}$ gradually decreases from 0 to −0.19. Between t = 251 and 260, parameter $\overline{F}$ gradually increases from −0.19 to 0. Right panel: Between t = 241 and 250, parameter $\overline{F}$ gradually decreases from 0 to −0.217. Between t = 251 and 260, parameter $\overline{F}$ gradually increases from −0.217 to 0.

not too high, it is clear that they allow certain agents to realize fraudulent profits. In the right panel of Figure 7, we assume that parameter σ_f^2 gradually increases from 3 to 7 between t = 251 and 500, while parameter σ_f^2 gradually decreases from 7 to 3 between t = 501 and 750. Parameter $\overline{F}$ is equal to 0. As it can be seen, fake news campaigns that target parameter σ_f^2 may also create exploitable crashes. Of course, such bubbles and crashes may have further repercussions. For instance, the banking sector of an economy may suffer from a sharp crash, putting the whole economy at risk. Clearly, policymakers need to be aware of the potential dangers associated with fake news campaigns.

Figure 8 illustrates how fake news campaigns can trigger abrupt (flash) crashes.[10] In the left panel of Figure 8, we observe a scenario where a fake news

10 As recounted by Karppi and Crawford (2016), on Tuesday, April 23, 2013, at 1:07 PM ET, a tweet with the alarming message "Breaking: Two Explosions in the White House and Barack Obama is injured" surfaced on the official Associated Press Twitter account. Within mere moments, the S&P experienced a staggering loss of approximately $136 billion. The swift dissemination of the tweet quickly revealed itself to be the result of a malicious hack of the Associated Press Twitter account. Mirroring the rapid onset of the crash, the S&P swiftly rebounded to its prior position. Remarkably, this entire sequence of events unfolded in less than 5 min. See Jacob Leal et al. (2016) and Jacob Leal and Napoletano (2019) for a deeper analysis and modeling of flash crashes.

campaign gradually decrease parameter $\overline{F}$ from 0 to −0.19 between t = 241 and 250. Subsequently, between t = 251 and 260, the influence of the fake news campaign diminishes, and parameter $\overline{F}$ gradually returns to its base value. Given that parameter σ_f^2 equals 2, multiple attractors coexist, as discussed in Figures 5 and 6. Initially, the initial value combination causes the risky asset's price to converge to its steady state. However, due to the fake news campaign, the risky asset's price plummets from 96 to 86.71 between t = 240 and 271, before gradually recovering. Instead of returning to its steady state, the risky asset's price experiences endogenous fluctuations, remaining below its steady state on average. Similarly, in the right panel of Figure 8, we examine another fake news campaign that reduces parameter $\overline{F}$ from 0 to −0.217 between t = 241 and 250, only to return it to its base value between t = 251 and 260. Again, parameter σ_f^2 is set to 2. In contrast to the left panel of Figure 8, the initial value combination in this scenario leads to endogenous asset price dynamics. As a consequence of the fake news campaign, the risky asset's price drops from 94.68 to 84.98 between t = 240 and 265. Subsequently, the risky asset price recovers, eventually fluctuating around the same price level as before the onset of the fake news campaign. Accordingly, financial markets burdened with a lot of (unbiased) fake news could have potentially serious breakdowns if even slight systematic shifts in the perception of the dividend process emerge.

5 Conclusions

The goal of our paper was to explore how fake news may influence the behavior of risky asset markets. As a workhorse, we used the seminal asset-pricing model by Brock and Hommes (1998). In particular, we assumed that fake news interferes with agents' perception of the risky asset's dividend process and renders the use of the fundamental expectation rule more costly. Our starting point was that fake news pollutes the information landscape, blurring the prospects of firms and, consequently, inducing (large) shifts of forecasted dividend payments. As a result, trading in equities becomes more risky, an aspect that decreases the steady-state price of risky assets. Observe that, slightly paradoxically, this may also be true even if fabricated or otherwise inaccurate and misleading news has a positive tone because the additional uncertainty surrounding the stock always has negative effects.

By increasing the effective costs of fundamental trading, more agents opt for the technical trading rule in equilibrium, an aspect that tends to destabilize the dynamics of the risky asset market. Importantly, the transition from stable dynamics to unstable dynamics may occur abruptly because a tiny change in a model parameter may cause drastic asset price fluctuations. Due to this endogenous risk component, the price fluctuations of the risky asset are concentrated below the risky asset's steady-state price.

Our model can be of use to the policymaker, showing that the most harmful effects of fake news are mainly related to a perceived exaggerated volatility that impacts risk-averse traders, makes fundamental analysis more difficult and costly, and ultimately depresses prices. Moreover, more agents embrace the cheaper technical expectation rule in equilibrium, increasing the potential to endogenously sustain large price swings. As the pernicious effects of fake news is channeled mostly through volatility, it would perhaps be hard to offset the damage through debunking campaigns or the provision of different, and more accurate, news or interpretations, as this additional source is likely to further increase the volatility of the information available to traders, if for no other reason because there is yet another source to scan and digest. Perhaps this vicious circle can realistically only be broken if fact-checking and truthful news is issued by extremely trustworthy institutions. In this case, differential trust may allow agents to retain only some (accurate) news and discard the other (fake) news. In the context of our model, this would mean that the overall role of F_t is undermined. Otherwise, the impact of fake news, as documented in our paper, may heavily impact the dynamics of financial markets and encourage fraudulent behavior for monetary or political purposes.

Acknowledgment: Paolo Pellizzari has received funding from the European Union's Horizon 2020 research and innovation programme under the Marie Skłodowska-Curie grant agreement No 956107. We thank two anonymous referees for helpful comments.

Appendix A

We now prove Proposition 1. Let $M_t^C = N_{t+1}^C$, $B_t^C = A_{t+1}^C$ and $B_t^F = A_{t+1}^F$. The absence of exogenous shocks, i.e. $d_t = 0$ and $f_t = 0$, implies that $D_t = \overline{D}$ and $F_t = \overline{F}$. The dynamics of our model is then driven by the 10-dimensional first-order non-linear deterministic map:

$$M:=\begin{cases} P_t=\dfrac{P_{t-1}+M_{t-1}^C\chi\left(P_{t-1}-X_{t-1}\right)+\left(1-M_{t-1}^C\right)\phi\left(\dfrac{\overline{D}+\overline{F}-\lambda\sigma_t^2\overline{S}}{r}-P_{t-1}\right)+\overline{D}+\overline{F}-\lambda\sigma_t^2\overline{S}}{1+r} \\ \sigma_{P,t}^2=\upsilon\sigma_{P,t-1}^2+(1-\upsilon)\left(P_{t-1}-U_{t-1}\right)^2 \\ U_t=\mu U_{t-1}+(1-\mu)P_{t-1} \\ M_t^C=\dfrac{1}{1+\exp\left[\beta\left(B_t^F-B_t^C\right)\right]} \\ X_t=P_{t-1} \\ Y_t=X_{t-1} \\ V_t=U_{t-1} \\ W_t=V_{t-1} \\ \sigma_{P,t}^2=\sigma_{P,t-1}^2 \\ \tilde{\sigma}_{P,t}^2=\sigma_{P,t-1}^2 \end{cases}, \tag{28}$$

where X_t, Y_t, V_t W_t, $\sigma_{P,t}^2$, and $\tilde{\sigma}_{P,t}^2$ are auxiliary variables. Moreover,

$$\sigma_t^2=\sigma_d^2+\sigma_f^2+\upsilon\sigma_{P,t-1}^2+(1-\upsilon)\left(P_{t-1}-U_{t-1}\right)^2,$$

$$\tilde{\sigma}_t^2=\sigma_d^2+\sigma_f^2+\upsilon\tilde{\sigma}_{P,t-1}^2+(1-\upsilon)\left(X_{t-1}-V_{t-1}\right)^2,$$

$$\tilde{\tilde{\sigma}}_t^2=\sigma_d^2+\sigma_f^2+\upsilon\tilde{\tilde{\sigma}}_{P,t-1}^2+(1-\upsilon)\left(Y_{t-1}-W_{t-1}\right)^2,$$

$$B_t^C=\frac{\left(X_{t-1}+\chi\left(X_{t-1}-Y_{t-1}\right)+\overline{D}+\overline{F}-(1+r)P_{t-1}\right)\left(\overline{D}-\overline{F}+2P_t-(1+r)P_{t-1}-X_{t-1}-\chi\left(X_{t-1}-Y_{t-1}\right)\right)}{2\lambda\sigma_t^2},$$

$$B_t^F=\frac{\left(X_{t-1}+\phi\left(\frac{\overline{D}+\overline{F}-\lambda\tilde{\sigma}_t^2\overline{S}}{r}-X_{t-1}\right)+\overline{D}+\overline{F}-(1+r)P_{t-1}\right)\left(\overline{D}-\overline{F}+2P_t-(1+r)P_{t-1}-X_{t-1}-\phi\left(\frac{\overline{D}+\overline{F}-\lambda\tilde{\sigma}_t^2\overline{S}}{r}-X_{t-1}\right)\right)}{2\lambda\tilde{\sigma}_t^2}$$
$$+\alpha\left(P_t-\frac{\overline{D}+\overline{F}-\lambda\sigma_t^2\overline{S}}{r}\right)^2-\left(c_1\sigma_d^2+c_2\sigma_f^2+c_3\left(\upsilon\sigma_{P,t-1}^2+(1-\upsilon)\left(P_t-U_{t-1}\right)^2\right)\right).$$

Setting $\overline{P}=P_t^\star=P_t=P_{t-1}=X_{t-1}=Y_{t-1}$, $\overline{\sigma_P^2}=\sigma_{P,t}^2=\sigma_{P,t-1}^2=\overline{\sigma_{P,t-1}^2}=\overline{\tilde{\sigma}_{P,t-1}^2}$, $\overline{U}=U_t=U_{t-1}=V_{t-1}=W_{t-1}$ and $\overline{N^C}=\overline{M^C}=M_t^C=M_{t-1}^C$, we find that map M possesses the unique steady state

$$\begin{aligned} S&=\left(\overline{P},\overline{\sigma_P^2},\overline{U},\overline{M^C},\overline{X},\overline{Y},\overline{V},\overline{W},\overline{\sigma_P^2},\overline{\tilde{\sigma}_P^2}\right) \\ &=\left(\frac{\overline{D}+\overline{F}-\lambda\left(\sigma_d^2+\sigma_f^2\right)\overline{S}}{r},0,\overline{P},\frac{1}{1+\exp\left[-\beta\left(c_1\sigma_d^2+c_2\sigma_f^2\right)\right]},\overline{P},\overline{P},\overline{P},\overline{P},0,0\right). \end{aligned} \tag{29}$$

Tedious computation reveals that the characteristic polynomial of the Jacobian matrix, evaluated at the steady state S, can be expressed by

$$P(\kappa) = \kappa^6 (\kappa - \upsilon)(\kappa - \mu)\left(\kappa^2 + a_1\kappa + a_2\right) \tag{30}$$

where $a_1 = \frac{(\phi-1)(1-\overline{N^C})-(1+\chi)\overline{N^C}}{1+r}$ and $a_2 = \frac{\overline{N^C}\chi}{1+r}$.

The characteristic polynomial gives rise to 10 eigenvalues. Since six eigenvalues are equal to zero, say $\kappa_1 = \kappa_2 = \kappa_3 = \kappa_4 = \kappa_5 = \kappa_6 = 0$, one eigenvalue is equal to υ, say $\kappa_7 = \upsilon$, and one eigenvalue is equal to μ, say $\kappa_8 = \mu$, the local stability of the steady state S hinges on the two remaining eigenvalues, say κ_9 and κ_{10}, determined by $\left(\kappa^2 + a_1\kappa + a_2\right) = 0$.[11] Necessary and sufficient conditions assuring that κ_9 and κ_{10} are less than one in modulus are given by (i) $1 + a_1 + a_2 > 0$, (ii) $1 - a_1 + a_2 > 0$, and (iii) $1 - a_2 > 0$. Conditions (i) and (ii) are always fullfilled.[12] Condition (iii) requires that

$$\overline{N^C}\chi < 1 + r. \tag{31}$$

Solving for $\beta\left(c_1\sigma_d^2 + c_2\sigma_f^2\right)$, we obtain

$$\beta\left(c_1\sigma_d^2 + c_2\sigma_f^2\right) < \log\left[\frac{1+r}{\chi - (1+r)}\right]. \tag{32}$$

A violation of this stability condition is associated with the emergence of a Neimark–Sacker bifurcation. See Medio and Lines (2001) for a review. Numerically, we can observe that a Neimark–Sacker bifurcation is either supercritical or subcritical. In the latter case, our simulations are consistent with the presence of a Chenciner bifurcation.

Appendix B

In this appendix, we investigate how the behavioral parameters β and χ influence the dynamics of our model. We maintain the same parameter setting configuration as presented in Table 1. For conciseness, our focus is on Case I and IV.

In Case I, the parameter σ_f^2 simply affects the perceived variance of the risky asset's dividend process, resulting in a decrease in its price without impacting its local stability. The top-left (top-right) panel of Figure 9 displays a bifurcation diagram depicting the risky asset's price (the market share of chartists) against the intensity of choice parameter β. While parameter β does not alter the steady-state price of the risky asset, which remains at $\overline{P} = 93$, an increase in parameter β leads to a rise in the steady-state market share of chartists. This is due to the lower costs associated with the technical trading rule compared to the fundamental trading rule. The steady state

11 Since $0 < \upsilon < 1$ and $0 < \mu < 1$, eigenvalues κ_7 and κ_8 do not comprise the local stability of the steady state S.

12 For completness, note that condition $(i)\ \frac{\phi(1-\overline{N^C})+r}{1+r} > 0$ and $(ii)\ \frac{2(1+\overline{N^C}\chi)-\phi(1-\overline{N^C})+r}{1+r} > 0$ always hold.

loses it local stability at $\beta \approx 2.398$, a value being considerably higher than $\beta = 1$ used in the benchmark setting. The bottom-left (bottom-right) panel of Figure 9 illustrates a bifurcation diagram showing the risky asset's price (the market share of chartists) versus the trend-extrapolation parameter χ. Parameter χ does not affect the steady-state price of the risky asset or the steady-state market share of chartists. However, an increase in chartists' extrapolation strength adversely impacts the stability of the risky asset market. Notably, the steady state loses it local stability at $\chi \approx 1.505$. Figure 9 suggests that we observe a supercritical Neimark-Sacker bifurcation. The amplitude of the dynamics starts small and then increases in accordance with the bifurcation parameters β and χ.

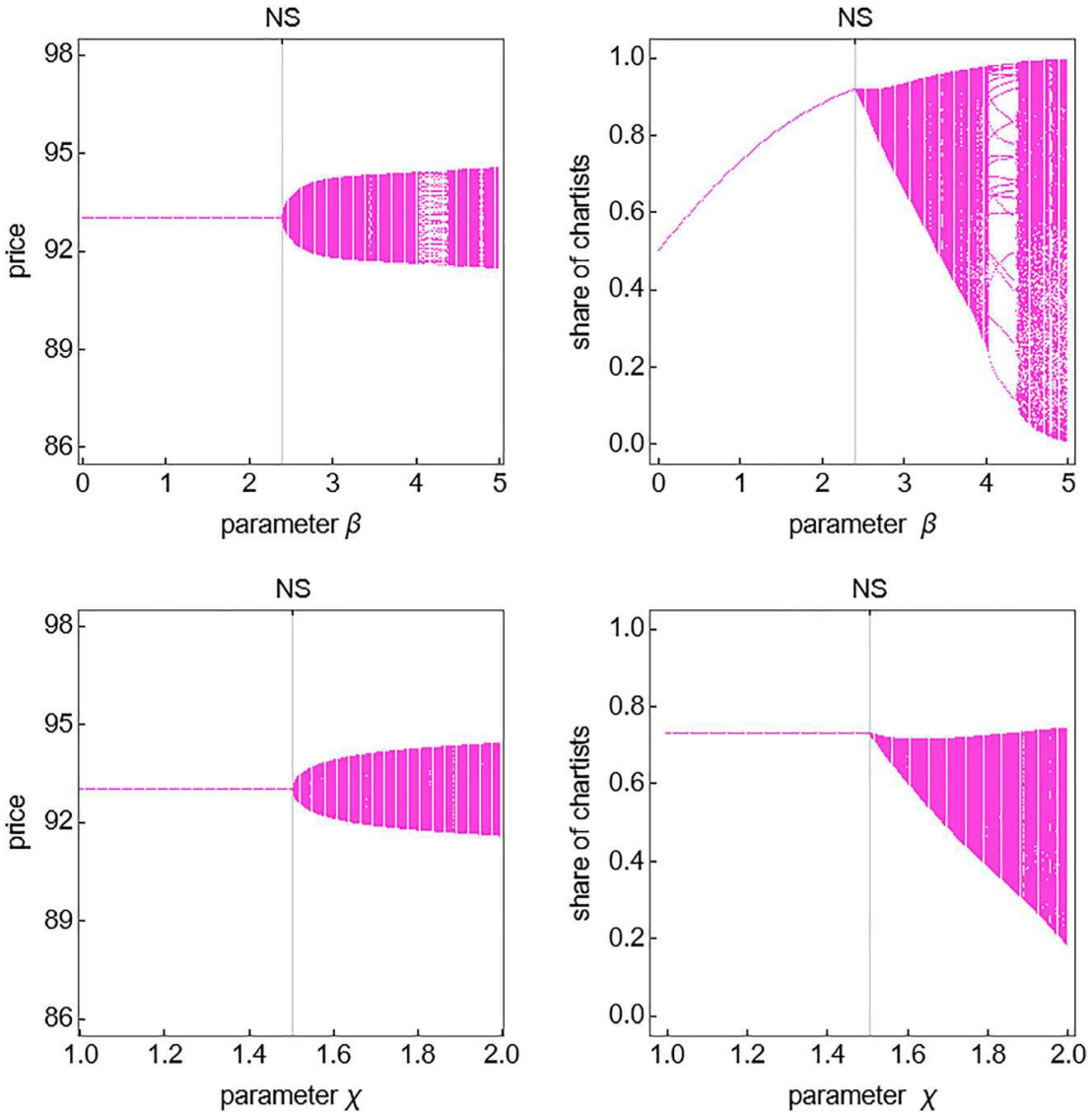

Figure 9: Robustness checks for Case I. The top panels display bifurcation diagrams depicting the risky asset's price (left) and the market share of chartists (right) against parameter β. The bottom panels illustrate the same for parameter χ.

Case IV encompasses our full model. The top-left (top-right) panel of Figure 10 displays a bifurcation diagram depicting the risky asset's price (the market share of chartists) against the intensity of choice parameter β. In this scenario, the steady-state loses its local stability at $\beta \approx 0.685$, being smaller than $\beta = 1$ used in the benchmark setting. The bottom-left (bottom-right) panel of Figure 10 presents a bifurcation diagram illustrating the risky asset's price (the market share of chartists) versus the extrapolation parameter χ. As predicted by Proposition 1, the steady-state loses its local-stability at $\chi \approx 1.133$. Figure 10 suggests that we now observe a subcritical Neimark–Sacker bifurcation. Unlike Case I, the transition between stable and endogenous fluctuations occurs abruptly.

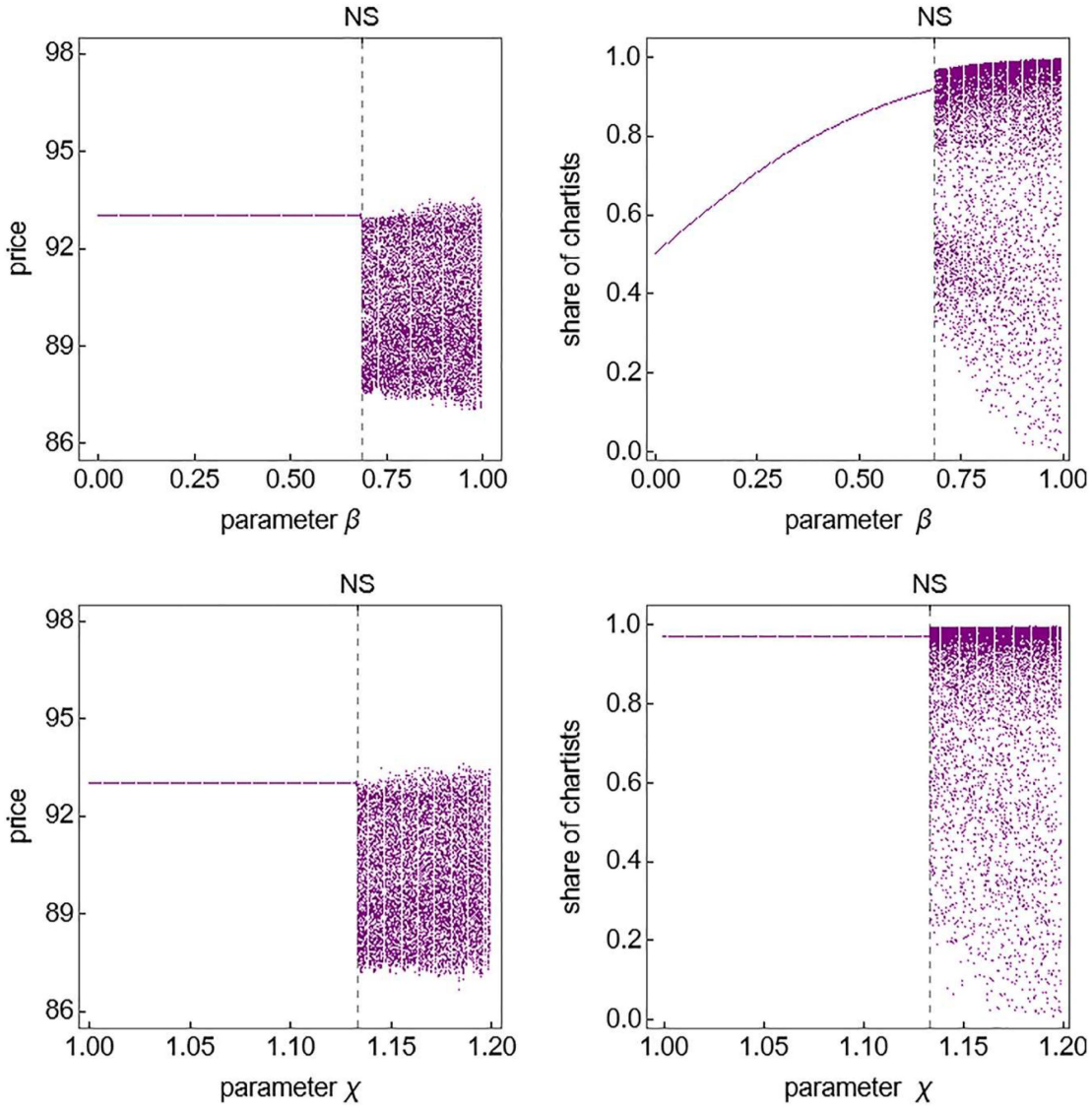

Figure 10: Robustness checks for Case IV. The top panels display bifurcation diagrams depicting the risky asset's price (left) and the market share of chartists (right) against parameter β. The bottom panels illustrate the same for parameter χ.

References

Agliari, A. 2006. “Homoclinic Connections and Subcritical Neimark Bifurcation in a Duopoly Model with Adaptively Adjusted Productions.” *Chaos, Solitons & Fractals* 29 (3): 739–55.

Allcott, H., and M. Gentzkow. 2017. “Social Media and Fake News in the 2016 Election.” *Journal of Economic Perspectives* 31 (2): 211–36.

Anufriev, M., and C. Hommes. 2012. “Evolutionary Selection of Individual Expectations and Aggregate Outcomes in Asset Pricing Experiments.” *American Economic Journal: Microeconomics* 4 (4): 35–64.

Anufriev, M., and J. Tuinstra. 2013. “The Impact of Short-Selling Constraints on Financial Market Stability in a Heterogeneous Agents Model.” *Journal of Economic Dynamics and Control* 37 (8): 1523–43.

Arcuri, M. C., G. Gandolfi, and I. Russo. 2023. “Does Fake News Impact Stock Returns? Evidence from US and EU Stock Markets.” *Journal of Economics and Business* 125: 106130.

Bao, T., J. Duffy, and J. Zhu. 2020. “Asset Pricing with Ambiguous Signals: An Experiment.” https://ssrn.com/abstract=3591779 (accessed July 16, 2024).

Bao, T., C. Hommes, and J. Pei. 2021. “Expectation Formation in Finance and Macroeconomics: A Review of New Experimental Evidence.” *Journal of Behavioral and Experimental Finance* 32: 100591.

Black, F. 1986. “Noise.” *The Journal of Finance* 41 (3): 528–43.

Boswijk, H. P., C. H. Hommes, and S. Manzan. 2007. “Behavioral Heterogeneity in Stock Prices.” *Journal of Economic Dynamics and Control* 31 (6): 1938–70.

Brock, W. A., and C. H. Hommes. 1998. “Heterogeneous Beliefs and Routes to Chaos in a Simple Asset Pricing Model.” *Journal of Economic Dynamics and Control* 22 (8): 1235–74.

Brock, W., C. Hommes, and F. Wagener. 2009. “More Hedging Instruments May Destabilize Markets.” *Journal of Economic Dynamics and Control* 33 (11): 1912–28.

Epstein, L. G., and M. Schneider. 2008. “Ambiguity, Information Quality, and Asset Pricing.” *The Journal of Finance* 63 (1): 197–228.

EUvsDisinfo. 2023. *Technical Report, East Stratcom Task Force. Technical Report, Euvsdisnfo Web Site*. Brussels: European External Action Service. https://euvsdisinfo.eu/ (Accessed July 18, 2024).

Fama, E. F. 1970. “Efficient Capital Markets: A Review of Theory and Empirical Work.” *The Journal of Finance* 25 (2): 383–417.

Franke, R., and F. Westerhoff. 2012. “Structural Stochastic Volatility in Asset Pricing Dynamics: Estimation and Model Contest.” *Journal of Economic Dynamics and Control* 36 (8): 1193–211.

Gaunersdorfer, A. 2000. “Endogenous Fluctuations in a Simple Asset Pricing Model with Heterogeneous Agents.” *Journal of Economic Dynamics and Control* 24 (5–7): 799–831.

Gaunersdorfer, A., and C. Hommes. 2007. “A Nonlinear Structural Model for Volatility Clustering.” In *Long Memory in Economics*, edited by G. Teyssière, and A. P. Kirman, 265–88. Berlin: Springer.

Gaunersdorfer, A., C. H. Hommes, and F. O. Wagener. 2008. “Bifurcation Routes to Volatility Clustering Under Evolutionary Learning.” *Journal of Economic Behavior & Organization* 67 (1): 27–47.

Hennequin, M., and C. Hommes. 2024. “Managing Bubbles in Experimental Asset Markets with Monetary Policy.” *Journal of Money, Credit and Banking* 56 (2–3): 429–54.

Hommes, C. H. 2006. “Heterogeneous Agent Models in Economics and Finance.” In *Agent-Based Computational Economics, Volume 2 of Handbook of Computational Economics*, edited by L. Tesfatsion, and K. Judd, 1109–86. Amsterdam: Elsevier.

Hommes, C. 2013. *Behavioral Rationality and Heterogeneous Expectations in Complex Economic Systems*. Cambridge: Cambridge University Press.

Hommes, C., H. Huang, and D. Wang. 2005. “A Robust Rational Route to Randomness in a Simple Asset Pricing Model.” *Journal of Economic Dynamics and Control* 29 (6): 1043–72.

Hommes, C, and D. in 't Veld. 2017. "Booms, Busts and Behavioural Heterogeneity in Stock Prices." *Journal of Economic Dynamics and Control* 80: 101–24.

Hommes, C., and F. Wagener. 2009. "Complex Evolutionary Systems in Behavioral Finance." In *Handbook of Financial Markets: Dynamics and Evolution*, edited by T. Hens, and K. R. Schenk-Hoppé, 217–76. Amstardam: Elsevier.

Jacob Leal, S., and M. Napoletano. 2019. "Market stability vs. market resilience: regulatory policies experiments in an agent-based model with low- and high-frequency trading." *Journal of Economic Behavior and Control* 15: 15–41.

Jacob, Leal, S., M. Napoletano, A. Roventini, and G. Fagiolo. 2016. "Rock around the clock : an agent-based model of low- and high-frequency trading." *Journal of Evolutionary Economics* 26 (1): 49–76.

Karppi, T., and K. Crawford. 2016. "Social Media, Financial Algorithms and the Hack Crash." *Theory, Culture & Society* 33 (1): 73–92.

Kogan, S., T. J. Moskowitz, and M. Niessner. 2023. "Social Media and Financial News Manipulation." *Review of Finance* 27 (4): 1229–68.

Lazer, D. M., M. A. Baum, Y. Benkler, A. J. Berinsky, K. M. Greenhill, F. Menczer, M. J. Metzger, et al. 2018. "The Science of Fake News." *Science* 359 (6380): 1094–6.

Liang, Y. 2022. "Learning from Unknown Information Sources." https://ssrn.com/abstract=3314789 (accessed July 18, 2024).

Lines, M., and F. Westerhoff. 2010. "Inflation Expectations and Macroeconomic Dynamics: The Case of Rational Versus Extrapolative Expectations." *Journal of Economic Dynamics and Control* 34 (2): 246–57.

Lines, M., and F. Westerhoff. 2012. "Effects of Inflation Expectations on Macroeconomic Dynamics: Extrapolative Versus Regressive Expectations." *Studies in Nonlinear Dynamics & Econometrics* 16 (4). https://doi.org/10.1515/1558-3708.1900.

Medio, A., and M. Lines. 2001. *Nonlinear Dynamics: A Primer*. Cambridge: Cambridge University Press.

Mignot, S., F. Tramontana, and F. Westerhoff. 2021. "Speculative Asset Price Dynamics and Wealth Taxes." *Decisions in Economics and Finance* 44: 641–67.

Neugart, M., and J. Tuinstra. 2003. "Endogenous Fluctuations in the Demand for Education." *Journal of Evolutionary Economics* 13: 29–51.

Scheufele, D. A., and N. M. Krause. 2019. "Science Audiences, Misinformation, and Fake News." *Proceedings of the National Academy of Sciences* 116 (16): 7662–9.

Shiller, R. J. 2017. "Narrative Economics." *American Economic Review* 107 (4): 967–1004.

Vosoughi, S., D. Roy, and S. Aral. 2018. "The Spread of True and False News Online." *Science* 359 (6380): 1146–51.